Intraseasonal interaction between the Madden–Julian Oscillation and the North Atlantic Oscillation

Christophe Cassou[1]

Bridging the traditional gap between the spatio-temporal scales of weather and climate is a significant challenge facing the atmospheric community. In particular, progress in both medium-range and seasonal-to-interannual climate prediction relies on our understanding of recurrent weather patterns and the identification of specific causes responsible for their favoured occurrence, persistence or transition. Within this framework, I here present evidence that the main climate intra-seasonal oscillation in the tropics—the Madden–Julian Oscillation[1,2] (MJO)—controls part of the distribution and sequences of the four daily weather regimes defined over the North Atlantic–European region in winter[3]. North Atlantic Oscillation[4] (NAO) regimes are the most affected, allowing for medium-range predictability of their phase far exceeding the limit of around one week that is usually quoted. The tropical–extratropical lagged relationship is asymmetrical. Positive NAO events mostly respond to a mid-latitude low-frequency wave train initiated by the MJO in the western–central tropical Pacific and propagating eastwards. Precursors for negative NAO events are found in the eastern tropical Pacific–western Atlantic, leading to changes along the North Atlantic storm track. Wave-breaking diagnostics tend to support the MJO preconditioning and the role of transient eddies in setting the phase of the NAO. I present a simple statistical model to quantitatively assess the potential predictability of the daily NAO index or the sign of the NAO regimes when they occur. Forecasts are successful in ~70 per cent of the cases based on the knowledge of the previous ~12-day MJO phase used as a predictor. This promising skill could be of importance considering the tight link[4] between weather regimes and both mean conditions and the chances of extreme events occurring over Europe. These findings are useful for further stressing the need to better simulate and forecast the tropical coupled ocean–atmosphere dynamics, which is a source of medium-to-long range predictability and is the Achilles' heel of the current seamless prediction suites[5–7].

Travelling synoptic pressure systems, or storms, contribute to a significant fraction of the daily to interannual variability of the extratropical climate. They are associated with the unstable nature of the upper-level westerly jet stream, and feed circulation patterns of larger scale (weather regimes) in which they are embedded. These regimes can be interpreted as quasi-stationary atmospheric circulations[8] during which the character of the synoptic storms is unusually persistent[9]. They are spatially well defined (typically the width of the oceanic basin) and limited in number; they ideally correspond to statistical-dynamical equilibria in phase space[10]. Objective analyses based on clustering techniques are often used to identify number, spatial structure and frequency of occurrence of weather regimes. The partition algorithm[11] I apply to daily maps of geopotential height

(Supplementary Information) leads to four circulation patterns estimated from extended boreal winter days (November–March) over 1974–2007 and over a broad North Atlantic–European domain (Fig. 1).

In agreement with previous studies[3,4], the two first regimes can be viewed as the negative and positive phases of the NAO (NAO− and NAO+, respectively), which can essentially be considered a measure of the variability of the zonal flow over the North Atlantic. The third regime is named Atlantic ridge and the fourth is often referred to as Scandinavian blocking (SBL). Links between flow regimes and mean conditions over Europe have been documented from daily[12,13] to decadal timescales[14]. The chances of extreme events (cold outbreak, heavy rainfall) occurring are also related to the four weather patterns (Supplementary Fig. 2), suggesting that a large part of the statistical distribution for surface variables, even regionally, could be assessed through the weather regime model.

A similar approach in weather-type classes has recently been applied in the tropics to describe and monitor in real time the dominant mode of intraseasonal climate variability, the MJO[1]. This is a natural component of the tropical coupled ocean–atmosphere system, and is characterized by a planetary-scale alternation of wet and dry periods associated with several changes in both tropical and subtropical atmospheric dynamics[2]. The MJO packet propagates eastwards around the globe with a typical 30–70-day cycle. By combining real-time satellite outgoing long-wave radiation (OLR, used as a proxy for convection) and atmospheric dynamical fields from operational reanalysis, it is possible to partition the daily MJO activity into eight intrinsic phases of 7–8-day nominal persistence[15] (Supplementary Information). These phases or classes can be interpreted as the tropical analogues of the extratropical weather regimes, except that regimes have episodic behaviour due to dominant chaos at mid latitudes whereas the time evolution of the MJO phases is mostly oscillatory.

MJO wintertime composites determined from November–March daily maps over 1974–2007 as for weather regimes show (Fig. 2) that the eastwards displacement of the anomalous OLR pattern is associated with significant modifications of the upper-level atmospheric circulation, interpreted as an equatorial Rossby–Kelvin wave response to anomalous tropical heating[16]. Those changes are characterized by vorticity couplets straddling the Equator and either collocated or shifted slightly westwards with respect to the anomalous convection cores and associated large-scale ascent or descent (Supplementary Fig. 3). Note that although OLR signals become weak when the MJO moves to the Western Hemisphere, these anomalous vorticity and divergence patterns clearly remain significant (for example, see Fig. 2, phases 2–3 and 6–7) and truly make manifest the planetary nature of the tropical intraseasonal oscillation.

[1]CNRS-Cerfacs, Global Change and Climate Modelling project, 42 Avenue G. Coriolis, 31057 Toulouse, France.

Extratropical responses to MJO kicks have been extensively described[16–19]. In this study, I adopt a novel approach more relevant to forecasting issues, and combine both tropical and extratropical clusters to investigate how the MJO influences the known and independent North Atlantic modes on medium-range timescales. For the eight MJO phases and for lags of up to +15 days (MJO in advance), I count the number of occurrences of each weather regime and
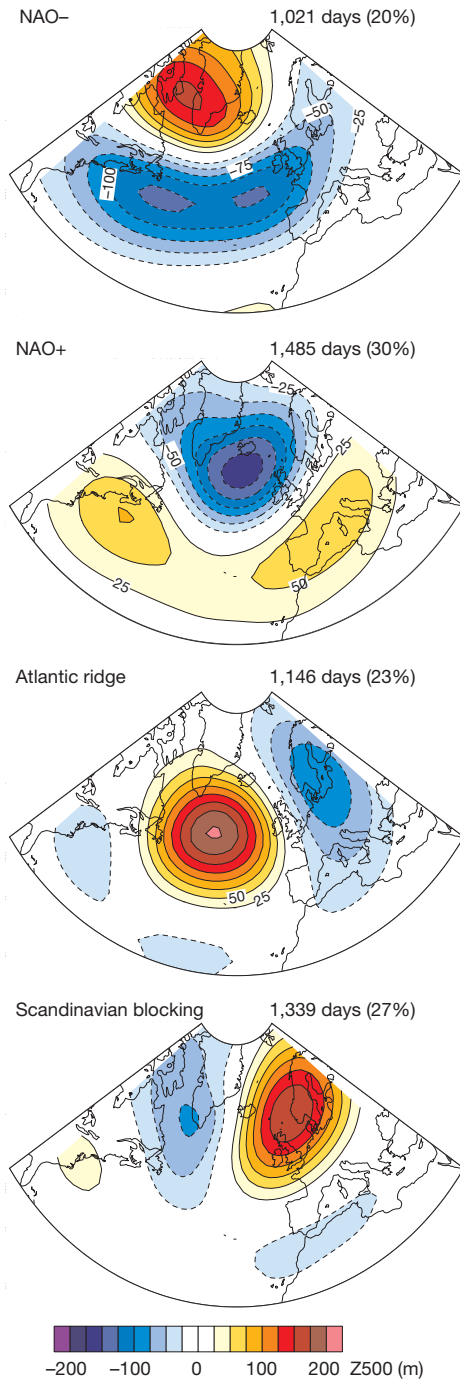
compare this number to its mean (Fig. 3). The relationship between phase 1 of the MJO and the occurrence of the four weather regimes is marginally significant. By contrast, the other MJO phases strongly suggest a significant tropical forcing upon the North Atlantic dynamics. For instance, phase 3 is not discriminative for the NAO
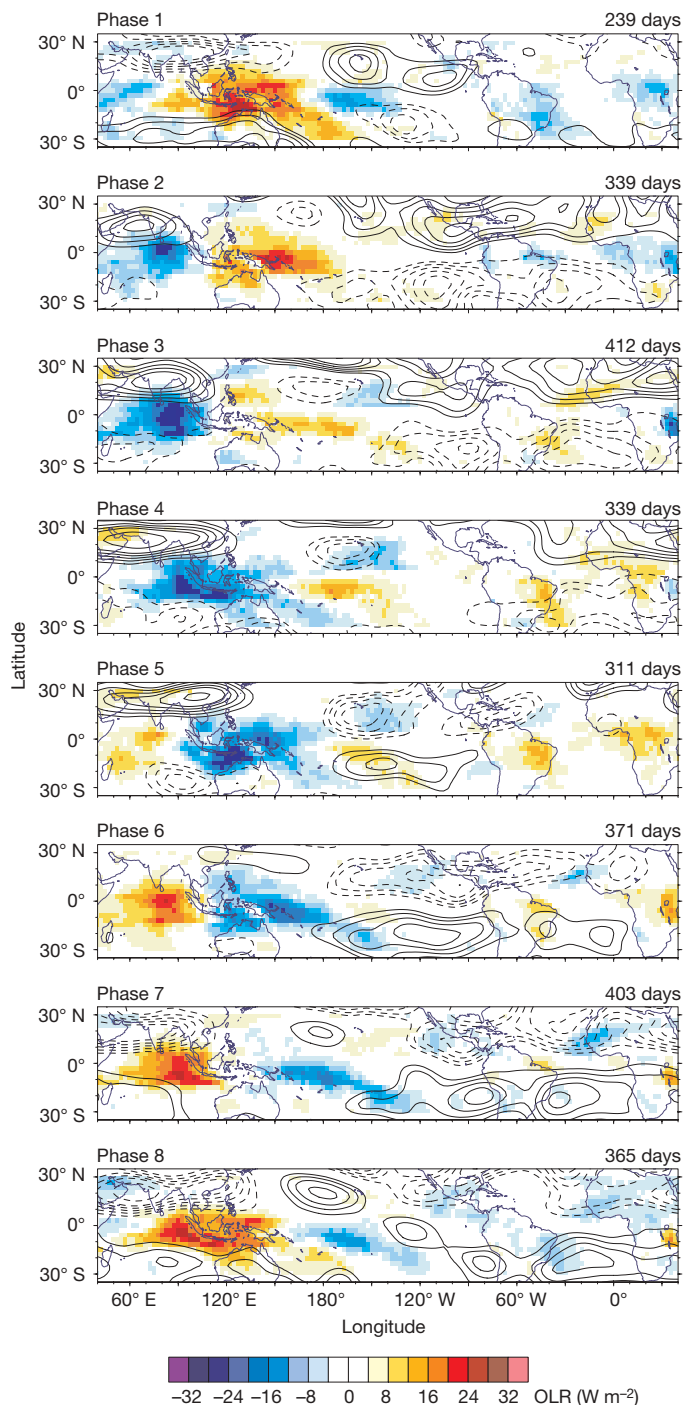

Figure 1 | Wintertime North Atlantic weather regimes. Centroids of the four weather regimes obtained from daily anomalous geopotential height at the 500-hPa altitude (Z500, colour) from the National Center for Environmental Prediction/National Center for Atmospheric Research (NCEP/NCAR) Reanalysis. Each percentage corresponds to the stated number of days and represents the mean frequency of occurrence of the regime computed over 1974–2007 from 1 November to 31 March. Contour intervals are 25 m. Details on the algorithm used for clustering are given in the Methods Summary and Supplementary Information.

Figure 2 | Dynamical and thermodynamical signatures of the eight phases of the MJO. Wintertime composite of OLR (colour) and stream function anomalies at 300 hPa (PSI300, contours) for the eight phases. Only strong MJO cycles are retained, corresponding to the stated number of days for each phase (see Supplementary Information). Bluer colours correspond to enhanced convection activity and wetter conditions, and redder colours correspond to reduced convection activity and drier conditions. Shading intervals are 4 W m^{-2} for OLR. Contour intervals are 1×10^6 m^2 s^{-1} for PSI300, starting at $\pm 2 \times 10^6$ m^2 s^{-1}. Positive values (solid) in the Northern Hemisphere and negative values (dashed) in the Southern Hemisphere represent anomalous anticyclonic circulation.
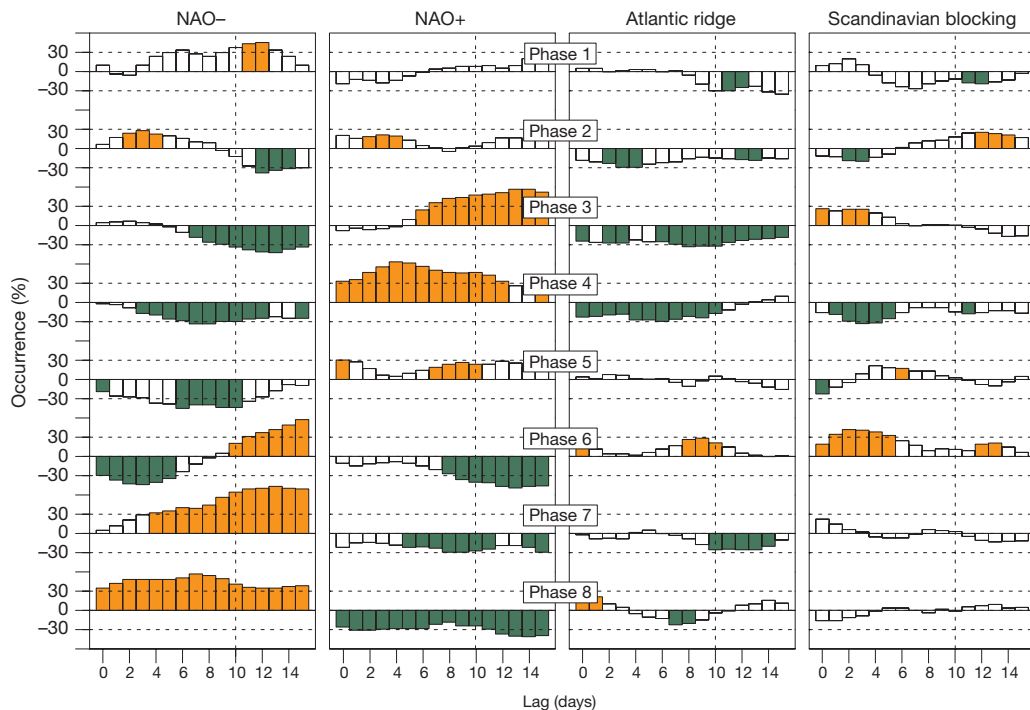
Figure 3 | Lagged relationships between the eight phases of the MJO and the four North Atlantic weather regimes. Table of contingency between the MJO phases (rows) and the North Atlantic weather regimes (columns). For each MJO phase, I plot the anomalous percentage occurrence of a given regime as a function of lag in days (with regimes lagging MJO phases). The 0% value means that the MJO phase is not discriminative for the regime whose occurrence is climatological. A 100% value would mean that this regime occurs twice as frequently as its climatological mean; −100% means no occurrence of this regime. The presence of a slope as a function of lag is suggestive of the MJO forcing. For white bars, either the change in the distribution between the four regimes is not significant on the basis of χ^2 statistics at the 99% significance level, or the individual anomalous frequency of occurrence is lower than the minimum significant threshold tested at 95% using a Gaussian distribution (approximation for binomial distribution because of the sufficiently large sampling). For orange and green bars, the regimes occur significantly more or, respectively, less frequently than their climatological occurrences.

regimes at lag 0, whereas ~10 days later the probability of a NAO− event occurring is reduced by ~40% and is mostly compensated for by an increase of ~60% in the probability of NAO+. The opposite is found for phase 6, which shows an increase of NAO− occurrence probability building up to ~70% for lags greater than 10 days, with NAO+ less probable. The Atlantic ridge regime seems to be less affected by the progress of the MJO, its occurrence being simply reduced by construction when NAO+ or NAO− regimes are dominant (phases 3–4 and 7, respectively). SBL occurrence is also weakly altered, except at short lag time in phase 6 (enhanced excitation) before NAO− maturation. The changes in the regime distribution occur progressively in accordance with the nominal 7–8-day persistence of the eight MJO phases.

Thus, Fig. 3 constitutes a contingency table providing evidence that phases 3 and 6 of the MJO can be interpreted as precursors of NAO+ and NAO− regimes, respectively. Lagged composites for these two specific phases reveal a clear asymmetry in the tropical forcing upon the two regimes. The days following phase 3 (Fig. 4a) are dominated by a mid-latitude low-frequency anomalous wave train that originates in the eastern Pacific, stretches across the North American continent and propagates eastwards following the Northern Hemispheric waveguide. Its penetration along the North Atlantic mean storm track (40°–60° N) is associated with dominant anticyclonic synoptic-scale wave breakings (AWBs) known as precursors for NAO+[20,21] from a lag of +6 days onwards (Fig. 4c), which is consistent with the response to the local modified background flow and the upstream shift towards the Equator of the tail end of the Pacific storm track[21,22] (Supplementary Fig. 5). The opposite picture emerges in the days following phase 6 of the MJO. There is no signal coming from the Pacific (Fig. 4b); height anomalies originating from Europe and propagating westwards are found instead from a lag of 0

to +6 days, before the development of a quasi-standing pattern projecting on NAO−. The proportion of AWBs is then clearly reduced from a lag of +6 days onwards (Fig. 4d). This reduction is almost entirely controlled by very high-frequency transients, which is consistent with the preferred *in situ* development of NAO− events[23] associated with more frequent cyclonic wave breakings[20,21] (CWBs), and contrasts with NAO+ events, in which intermediate-frequency eddy activity has a role[23] (difference between the purple and green curves in Fig. 4c).

The precursory wave train for NAO+ is initiated in the western–central Pacific (phases 2–3) in response to the direct MJO forcing following forced Rossby wave theories (Supplementary Fig. 6). Processes for teleconnection between MJO and NAO− regimes appear to be less straightforward. Two non-exclusive mechanisms are proposed. SBL regimes are present at short lag time in phase 6 (Fig. 3) and may subsequently trigger the onset of NAO− events[24,25]. This hypothesis is consistent with the retrograde propagation of height anomalies[23] (Fig. 4b). The enhanced occurrence of SBL in phase 6, and consequently NAO− at greater lags, can be interpreted as the consequence of previous NAO+ excitation (phases 4–5), considering that the preferred transitions between regimes follow the route NAO+ to SBL to NAO−[3] (Supplementary Information). The hypothesis is based on evidence that the extratropical atmosphere retains information about regime occurrences over medium-range timescales[3]. In this case, enhanced NAO− in late phase 6 and phase 7 would not be directly forced by the MJO, but would correspond to the timescale resonance between the eastward propagation of the MJO and the preferred sequence of the North Atlantic regimes.

The second mechanism proposed for teleconnection between MJO and NAO− relies on direct tropical forcings originating from the
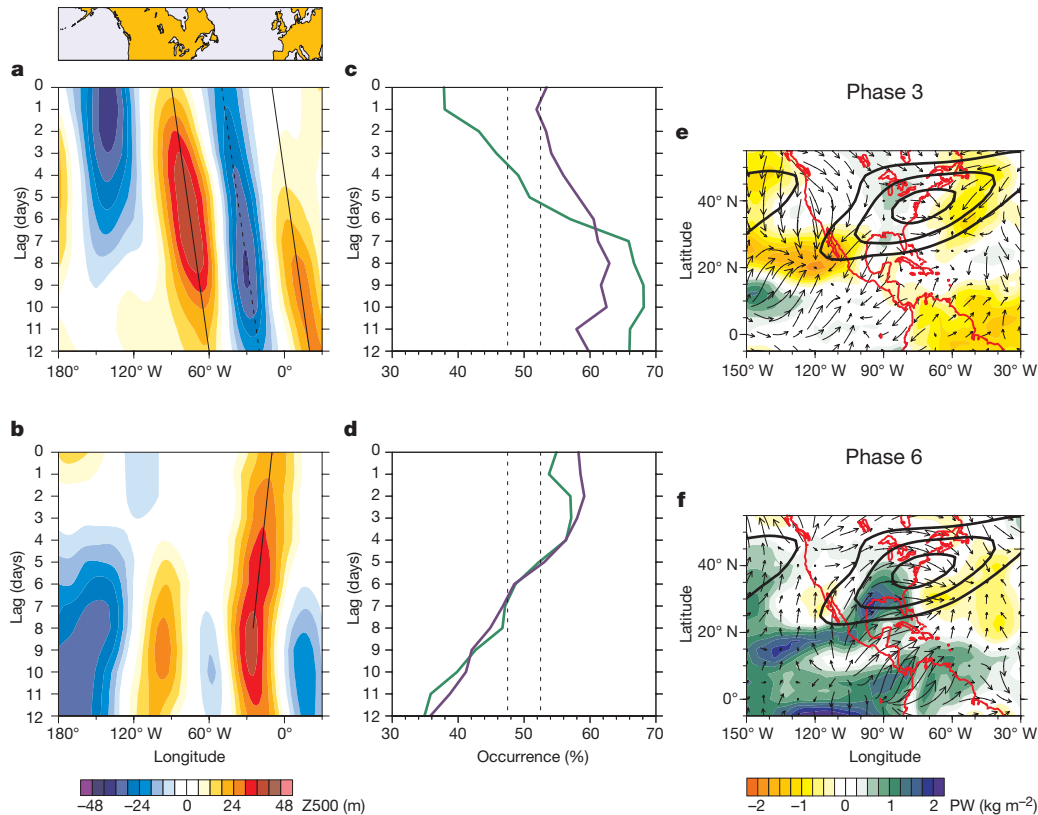
Figure 4 | Asymmetrical tropical–extratropical connection between two specific phases of the MJO leading to NAO+ and NAO− events.
a, **b**, Longitude–time plots of lagged composites of daily Z500 (colour) anomalies averaged between $40°$ N and $60°$ N for phases 3 and 6 of the MJO, respectively. **c**, **d**, Percentage occurrence of AWB as a function of lag for phases 3 and 6, respectively. Wave breakings are assessed from a daily index of meridional eddy momentum flux, band-pass filtered either for 2–6 days (very high frequency, purple) or for 2–12 days (intermediate plus very high frequency, green), and averaged along the Atlantic storm track ($100°–10°$ W, $30°–60°$ N). Positive and negative values of this index respectively stand for AWB and CWB[22]. The percentage occurrence of AWB is thus computed as the ratio of AWB days to the total sample. Significance at 95% is tested using a Monte Carlo method (1,000 resamplings) and indicated by the two dashed lines. **e**, **f**, Composites of anomalous 300-hPa divergent wind (arrows) and precipitable water (PW, colour) averaged from lags from 0 to +5 days, for phases 3 and 6, respectively. Shading intervals are $0.25 \, \text{kg m}^{-2}$ for precipitable water. The contours represent the mean climatological jet stream (zonal wind at 300 hPa). Contour intervals are $6 \, \text{m s}^{-1}$, starting at $22 \, \text{m s}^{-1}$.

eastern Pacific. At short lag time, although the anomalous convection is weak (Fig. 2), phase 6 is associated with tropical upper-level divergence around $120°$ W (the signal is just as strong as for phase 3 over Indonesia, as indicated in Supplementary Fig. 3) and is compensated to the northeast by convergence both at the entrance to, and the southern flank of, the mean climatological jet stream (Fig. 4f). The local Hadley cell is intensified[26], leading to advection of absolute vorticity by the MJO divergent tropical outflow (Fig. 4f) and to enhanced momentum convergence around $30°$ N. This picture is consistent with there being a Rossby wave source[27] around $20°$ N, $110°$ W (Supplementary Fig. 6) that initiates a downstream wave train propagating northeastwards towards Europe following a preferred curving path (not shown) in line with several studies[16,28]. Note that, concurrently, enhanced precipitable water extends from the tropical eastern Pacific to the entrance of the jet stream during phase 6, consistent with the upper-tropospheric anomalous circulation. There is evidence[22] that destabilized atmosphere due to enhanced moisture located upstream from the North Atlantic storm track favours CWBs in agreement with our findings, and could thus be an additional contributor to NAO− occurrence. Opposite phenomena (Fig. 4e) tend to appear for phase 3 (upper-level convergence at $\sim110°$ W, tendency towards drier atmosphere at the entrance of the jet stream), although signals are significantly weaker.

In summary, I show that forced Rossby waves initiated by the MJO either in the western Pacific (NAO+ precursors) or in the eastern Pacific (NAO− precursors) should be interpreted as a modification of the background flow[29] or catalysts for a full development of NAO

regimes that involves a strong interaction with transient eddies by means of wave breaking.

These results contribute to the window of opportunity for enhanced predictive skill of the wintertime NAO at medium-range timescales. As a crude estimate, I built the most simple generalized linear model[30] using MJO phases as predictors (Supplementary Information). The probability of predicting the correct sign of the NAO regimes when they occur is $\sim70\%$ at a lead time of +9 to +13 days (Supplementary Figs 7–8). A similar accuracy is obtained using the NAO index subdivided into terciles. These significant values should be treated as benchmarks for numerical weather prediction models and mean that there is some predictability far exceeding the limit of around one week that is usually quoted as the limit for the North Atlantic–European sector. On the basis of my findings, I suggest that the next step towards improving our capabilities in forecasting on the timescale of 5–30 days can be summarized in three main points. First, it is essential to get very accurate real-time information on the three dimensional tropical atmospheric dynamics and thermodynamics for the model initialization step. Second, it is crucial to be able to correctly simulate and forecast the evolution or persistence of the initialized MJO dynamics that is somehow achieved using statistical models[7] but which is far from being possible with the current generation of weather[5] and climate models[6,7]. Last, it is important to correctly simulate the tropical–extratropical atmospheric bridges from daily to seasonal timescales. This requires a good representation of the atmospheric mean state and transient eddy activity, upon which the latitudinal connection is dependent.

METHODS SUMMARY

North Atlantic weather regimes. The k-means clustering algorithm is applied to anomalous daily geopotential height at 500 hPa from the NCEP/NCAR Reanalysis to obtain four weather regimes over a large North Atlantic–Europe domain. The decomposition is limited to the 90° W–30° E, 20°–80° N region and performed in the empirical-orthogonal-function phase space to speed up the computation (14 modes retained, corresponding to 90% of variance). A cosine weight as a function of latitude is applied to the data and the climatology is computed over 1974–2007 for winter days (November–March). Daily attribution to a given weather pattern is based on a minimum-Euclidean-distance criterion. The optimal number of regimes, k, is chosen on the basis of Brownian noise statistics[11].

MJO. The MJO activity is assessed through the real-time multivariate MJO index (RMMI)[15] provided daily and operationally by the Australian Bureau of Meteorology. Only active MJO phases (RMMI amplitude greater than one) are retained throughout the entire study.

MJO–North Atlantic coupling. Statistical evidence of interaction between the MJO and North Atlantic regimes is simply assessed through lagged composites between the MJO phases (in advance) and the North Atlantic regimes. Significance for contingency is based on χ^2 and Gaussian statistics to test respectively for changes in the combined four-regime distribution and for individual anomalous occurrences as a function of lag in days. The physical mechanisms supporting the asymmetrical MJO–NAO connection are extracted from lagged composites for several dynamical fields from the NCEP/NCAR Reanalysis. Diagnostics for wave breaking are obtained from meridional eddy momentum fluxes computed daily over the North Atlantic along the storm track, and analysed in two bands of frequency based on Lanczos filtering.

1. Madden, R. A. & Julian, P. R. Observations of the 40–50 day tropical oscillation. *Mon. Weath. Rev.* **112,** 1109–1123 (1994).
2. Zhang, C. Madden-Julian oscillation. *Rev. Geophys.* **43,** doi:10.1029/2004RG000158 (2005).
3. Vautard, R. Multiple weather regimes over the North Atlantic: Analysis of precursors and successors. *Mon. Weath. Rev.* **118,** 2056–2081 (1990).
4. Hurrell, J. W., Kushnir, Y., Ottersen, G. & Visbeck, M. in *North Atlantic Oscillation: Climate Significance and Environmental Impact* (eds Hurrell, J. W., Kushnir, Y., Ottersen, G. & Visbeck, M.) 1–35 (Geophys. Monogr. 134, American Geophysical Union, 2003).
5. Vitard, F., Woolnough, S., Balmaseda, M. A. & Tompkins, A. M. Monthly forecast of the Madden-Julian Oscillation using a coupled GCM. *Mon. Weath. Rev.* **135,** 2700–2715 (2007).
6. Lin, J.-L. *et al.* Tropical intraseasonal variability in 14 IPCC AR4 climate models. Part I: convective signals. *J. Clim.* **19,** 2665–2690 (2006).
7. Waliser, D. *et al.* The experimental MJO prediction project. *Bull. Am. Meteorol. Soc.* **87,** 425–431 (2006).
8. Reinhold, B. & Pierrehumbert, R. Dynamics of weather regimes: quasi-stationary waves and blocking. *Mon. Weath. Rev.* **110,** 1105–1145 (1982).
9. Straus, D., Corti, S. & Molteni, F. Circulation regimes: chaotic variability versus SST-forced predictability. *J. Clim.* **20,** 2251–2272 (2007).
10. Molteni, F., Kuscharski, F. & Corti, S. in *Predictability of Weather and Climate* (eds Palmer, T. & Hagedorn, R.) 365–389 (Cambridge Univ. Press, 2006).
11. Michelangeli, P., Vautard, R. & Legras, B. Weather regimes: recurrence and quasi-stationarity. *J. Atmos. Sci.* **52,** 1237–1256 (1995).
12. Philipp, A. *et al.* Long term variability of daily North Atlantic-European pressure patterns since 1850 classified by simulated annealing clustering. *J. Clim.* **20,** 4065–4095 (2007).
13. Slonosky, V. C. & Yiou, P. The North Atlantic Oscillation and its relationship with near surface temperature. *Geophys. Res. Lett.* **28,** 807–810 (2001).
14. Hurrell, J. W. Decadal trends in the North Atlantic Oscillation: Regional temperatures and precipitation. *Science* **26,** 676–679 (1995).
15. Wheeler, M. C. & Hendon, H. H. An all-season real-time multivariate MJO index: development of an index for monitoring and prediction. *Mon. Weath. Rev.* **132,** 1917–1932 (2004).
16. Matthews, A. J., Hoskins, B. J. & Masutani, M. The global response to tropical heating in the Madden-Julian Oscillation during northern winter. *Q. J. R. Meteorol. Soc.* **130,** 1991–2011 (2004).
17. Ferranti, L., Palmer, T. N., Molteni, F. & Klinker, E. Tropical-extratropical interaction associated with the 30–60 day oscillation and its impact on medium and extended range prediction. *J. Atmos. Sci.* **47,** 2177–2199 (1990).
18. Higgins, R. W. & Mo, K. C. Persistent North Pacific circulation anomalies and the tropical intraseasonal oscillation. *J. Clim.* **10,** 223–244 (1997).
19. Zhou, S. & Miller, A. J. The interaction of the Madden-Julian Oscillation and the Arctic Oscillation. *J. Clim.* **18,** 143–159 (2005).
20. Benedict, J. J., Lee, S. & Feldstein, S. B. Synoptic view of the North Atlantic Oscillation. *J. Atmos. Sci.* **61,** 121–144 (2004).
21. Franske, C., Lee, S. & Feldstein, S. B. Is the North Atlantic Oscillation a breaking wave? *J. Atmos. Sci.* **61,** 145–160 (2004).
22. Rivière, G. & Orlanski, I. Characteristics of the Atlantic storm track eddy activity and its relationship with the North Atlantic Oscillation. *J. Atmos. Sci.* **64,** 241–266 (2007).
23. Feldstein, S. B. The dynamics of NAO teleconnection pattern growth and decay. *Q. J. R. Meteorol. Soc.* **129,** 901–924 (2003).
24. Croci-Maspoli, M., Schwierz, C. & Davies, H. Atmospheric blocking: space-time links to the PNA. *Clim. Dyn.* **29,** 713–725 (2007).
25. Scherrer, S. C., Croci-Maspoli, M., Schwierz, C. & Appenzeller, C. Two dimensional indices of atmospheric blocking and their relationship with winter climate patterns in the Euro-Atlantic region. *Int. J. Climatol.* **26,** 233–249 (2006).
26. Tyrrell, G. C., Karoly, D. J. & McBride, J. L. Links between tropical convection and variations of the extratropical circulation during TOGA-CORE. *J. Atmos. Sci.* **53,** 2735–2748 (1996).
27. Sardeshmukh, P. & Hoskins, B. The generation of global rotational flow by steady idealized tropical divergence. *J. Atmos. Sci.* **45,** 1228–1251 (1988).
28. Hoskins, B. J. & Ambrizzi, T. Rossby wave propagation on a realistic longitudinally varying flow. *J. Atmos. Sci.* **50,** 1661–1671 (1993).
29. Woollings, T., Hoskins, B., Blackburn, M. & Berrisford, P. A new Rossby wave-breaking interpretation of the North Atlantic Oscillation. *J. Atmos. Sci.* **65,** 609–626 (2008).
30. Simon, S. J. & Baddour, O. in *Seasonal Climate: Forecasting and Managing Risk* (eds Troccoli, A., Harrison, M., Anderson, D. L. T. & Mason, S. J.) 163–201 (Springer, 2008).